THE ASTROPHYSICAL JOURNAL, 420:L57–L61, 1994 January 10

X-RAY BUMPS, IRON Kα LINES, AND X-RAY SUPPRESSION BY OBSCURING TORI IN SEYFERT GALAXIES

JULIAN H. KROLIK
Department of Physics & Astronomy, JHU, Homewood Campus, Baltimore, MD 21218
PIERO MADAU
Space Telescope Science Institute, 3700 San Martin Drive, Baltimore, MD 21218
AND
PIOTR T. ŻYCKI
Observatoire de Paris-Meudon, 92195 Meudon, France[1]
Received 1993 September 10; accepted 1993 October 25

ABSTRACT

We investigate the X-ray spectral properties of unobscured type 1 and obscured type 2 Seyferts as predicted by the unified Seyfert scheme. We consider the reprocessing of X-ray photons by photoelectric absorption, iron fluorescence, and Compton downscattering in the obscuring tori surrounding these active nuclei, and compute by Monte Carlo methods the reprocessed spectra as a function of the viewing angle. Depending on the optical depth and shape of the torus, and on the viewing angle, the X-ray flux can be suppressed by substantial factors when our line of sight is obscured. We show that an immediate consequence of the existence of an obscuring thick torus is the production in the spectra of type 1 Seyfert galaxies of a bump in the continuum above 10–20 keV and an Fe Kα line with significant equivalent width. In those type 2 Seyferts for which the hard X-ray spectrum has been substantially suppressed, the equivalent width of the Fe Kα line in the transmitted spectrum can be very large.

Subject headings: diffuse radiation — galaxies: Seyfert — quasars: general — X-rays: galaxies

1. INTRODUCTION

In recent years much observational evidence has accumulated in support of the unified Seyfert scheme, according to which an opaque torus, at a distance of several to several tens of parsecs from the central source, occults the majority of solid angle around Seyfert nuclei (Antonucci 1993). Antonucci & Miller (1985) clearly demonstrated that the archetypical type 2 Seyfert galaxy, NGC 1068, hides a type 1 nucleus in its center. Their spectropolarimetric observations showed that obscuring matter, probably having toroidal geometry, blocks our line of sight to the nucleus. When our view is occulted by the torus, photons of all energies from the far-infrared to at least several keV are blocked, and in these bands we can only detect the Seyfert 1 nucleus indirectly, via electron scattering from a warm, ionized medium located above the axis of the obscuring torus. We then see it as a Seyfert 2. Since then, Miller & Goodrich (1990) showed that the same situation obtains in many other type 2 Seyferts. Additional evidence for a toroidal geometry comes from the cones of high ionization line emission observed in Seyfert galaxies (see, e.g., Wilson, Ward, & Haniff 1988; Pogge 1988), perhaps the most direct evidence for small-scale collimation of the optical/UV nuclear emission.

The obscuration hypothesis is supported by X-ray studies of Seyfert galaxies. Type 1 Seyfert emit nearly as much energy in the X-ray band as anywhere else in the spectrum. On the other hand, most type 2 Seyfert galaxies are weak in X-rays, particularly at a few keV. In a UV-selected sample of type 2 Seyfert observed with *Ginga*, Mulchaey, Mushotzky, & Weaver (1992) found that in most cases the hard X-ray flux is a significant fraction of the bolometric flux, but that photons softer than several keV are absent. They inferred absorbing columns ranging from 3×10^{22} cm^{-2} to more than 10^{24} cm^{-2}. Because many type 2 Seyferts were not detected by *Ginga* (Awaki & Koyama 1994), although X-ray fluxes comparable to their infrared fluxes would have been, it is likely that the obscuring torus in these cases is optically thick to Compton scattering, i.e., $N_{\rm H} >$ few $\times 10^{24}$ cm^{-2}. Moreover, as predicted on the basis of the obscuration/reflection model (Krolik & Kallman 1987), observed Kα lines have extremely large equivalent widths ($\sim$1.5 keV) in NGC 1068 and NGC 4945 (Elvis & Lawrence 1988; Koyama et al. 1989; Awaki & Koyama 1992; Marshall et al. 1993). Lines of such large equivalent width can only be formed if the X-ray continuum striking the line emission region is much stronger than the continuum we see.

Ginga observations of Seyfert 1 galaxies in the 2–30 keV band (Pounds et al. 1990; Piro, Yamauchi, & Matsuoka 1990; Matsuoka et al. 1990) have also shown the presence of a flat component above 10 keV. This is generally explained, along with the Fe Kα line, by a reflection spectrum, in which an incident power law with $\alpha \sim 0.9$ is reflected towards the observer by cold gas close to the central compact object, e.g. an accretion disk. The impinging power law photons are photoelectrically absorbed at energies $\lesssim$10 keV. Compton downscattering at increasingly higher energies downgrades the photon energies to form a "reflected hump" in the albedo in the 2–100 keV band (Lightman & White 1988). If fitted with a power law only, the spectral index is $\alpha \sim 0.7$ in the 2–20 keV range, and $\alpha \sim 0.4$ in the 10–35 keV range (Pounds et al. 1990).

One-dimensional Monte Carlo calculations of active galactic nucleus (AGN) X-ray spectra transmitted through a thick spherical cloud have been recently performed by Madau, Ghisellini, & Fabian (1993) and Leahy & Creighton (1993). However, a toroidal belt of matter with Thomson depth order unity or more can be expected to create a substantial viewing

[1] On leave from Nicolaus Copernicus Astronomical Center, Bartycka 18, 00-716 Warsaw, Poland.

angle dependence in the observed X-ray flux. A preliminary exploration of these effects was made in Awaki et al. (1991). In this *Letter* we investigate this angle dependence quantitatively using a two-dimensional Monte Carlo code. As expected, we find that the X-ray flux in obscured directions is suppressed; however, we also find an alternative explanation for the X-ray bumps and Fe Kα lines seen in unobscured directions: reflection and fluorescence from the torus.

2. PROBLEM DEFINITION AND CALCULATION

To investigate the angle-dependent transfer effects, we choose the simplest geometry consistent with the problem: a torus filled with constant density material, having exact cylindrical symmetry and a cross section which is either square or rectangular. To obscure the nucleus at optical wavelengths, the torus must contain dust; if it is cold enough to allow dust to survive, its opacity to photons with energy greater than 0.5 keV must be essentially that of cold, neutral matter. Because the absolute intensity of the X-rays in the torus is irrelevant to the problem, its distance from the nucleus is also irrelevant; however, the ratio between its vertical thickness and its (cylindrical) inner radius is important because it defines the opening angle within which outside observers possess unobscured views of the nucleus. The ratio of obscured to unobscured solid angle can be estimated by counting the number of type 2 objects relative to type 1. Efforts to date indicate that the integrated space density of type 2 Seyferts is between 2 and 10 times larger than the density of Seyfert 1 galaxies (Phillips, Charles, & Baldwin 1983; Osterbrock & Shaw 1988; Huchra & Burg 1992). In the following, we set the half-opening angle of the torus $\theta = 30°$ (for a type 2:1 ratio $\simeq 6.5$). In order to treat the simplest possible case, in all but one of our simulations the torus was given a square cross section. However, to demonstrate the effect of geometry, we also ran one case whose equatorial thickness was twice as great as its vertical thickness.

One of our goals is to investigate the dependence of the observed spectra on the opacity of the blocking material. The interesting range of Thomson optical depths through the equatorial plane of the torus is $\tau_T \sim 0.1$–10. We will present calculations for $\tau_T = 0.5$, 1, 2, and 4. To illustrate the effects of obscuration we will use an incident continuum spectrum which is simply a power law with flux per unit energy $F_x \propto x^{-0.9}$, where x is the photon energy in electron mass units. Recent OSSE and *GRANAT* observations of Seyfert galaxies at energies above 50 keV (Cameron et al. 1994; Maisack et al. 1993; Fabian et al. 1993; Jourdain et al. 1992) indicate the presence of an exponential break with characteristic energy $\sim$50–100 keV; if this feature turns out to be generic, it will be easy to adjust our predictions from the effects shown in our figures.

The radiation transfer is computed with a Monte Carlo code constructed using the photon-escape weighting method of Pozdnyakov, Sobol', & Sunyaev (1983). We set the electron temperature T_e equal to zero, and consequently neglect Compton upscattering. The full Klein-Nishina scattering cross section is adopted, and the bound-free opacity associated with standard cosmic abundance material is taken from Morrison & McCammon (1983). Each simulation typically uses 10^7 photons.

3. UNOBSCURED VIEWS

On lines of sight with unobscured views of the nucleus, the X-rays received have had either of two histories: one set came directly from the nucleus, preserving the true spectral form of the emitted continuum; the other set were initially directed toward the torus, but were scattered by electrons within the torus into the line of sight. To have a significant probability of scattering, these photons must traverse a column density of at least $\sim 10^{24}$ cm^{-2}; consequently, the probability of any photon with initial energy $\lesssim 10$ keV surviving this trip is very small. On the other hand, photons with initial energy greater than 100 keV scatter in the Klein-Nishina regime. These, too, are underrepresented in the reflected flux because of three effects: the Klein-Nishina cross section declines with increasing energy, so their probability of scattering is smaller than for lower energy photons; the angular distribution of Klein-Nishina scattering is weighted toward forward-scattering; and photons of this energy which scatter against electrons and do change direction by a significant angle lose much of their energy to Compton recoil. The spectrum of X-rays emerging from the torus after at least one scatter is therefore depressed strongly below 10 keV and above 100 keV.

The shape of this reflection "bump" is illustrated in Figure 1 for $\tau_T = 1$ and 2. Also plotted in Figure 1 is the X-ray spectrum that would be seen if the same incident flux were radiated isotropically above a semi-infinite, flat, cold slab, as envisioned, for example by Lightman & White (1988). Many authors have suggested that the flattening frequently seen in AGN spectra at energies greater than 10 keV, along with the Fe Kα line, is due to just this sort of reflection from an adjacent accretion disk (Pounds et al. 1990; George, Nandra, & Fabian 1990; George & Fabian 1991). We draw the reader's attention to the close similarity in shape between the X-ray spectrum reflected by an obscuring torus and the "Compton reflection hump" from a cold disk. The amplitude of the bump is, of course, a decreasing function of torus opening angle.

Figures 2*a*–2*d* show how the contribution of this bump to the unobscured spectrum depends on the optical depth of the torus and the shape of the torus cross section. Note that, in unobscured directions, the received spectrum is independent of viewing angle. This is because the majority of the flux is direct, and independent of viewing angle by definition, while the intensity leaving the torus through its top surface (the only portion visible to an observer with an unobscured view) is

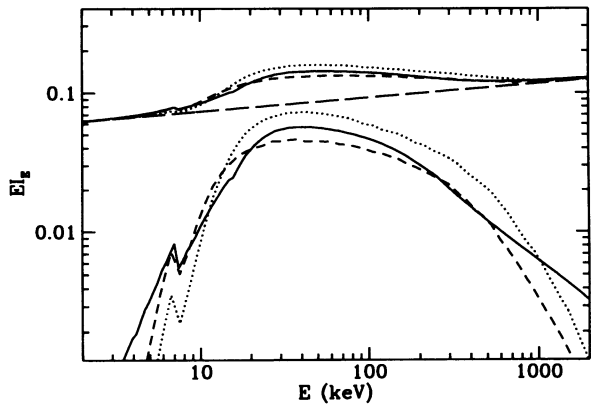

FIG. 1.—Reflected and composite (reflected + direct) spectra. The long-dashed line is the power law incident spectrum $F_E \propto E^{-0.9}$. The spectra observed from unobscured directions, obtained by Monte Carlo simulations, are shown for tori with square cross sections and optical depths $\tau_T = 1$(*short-dashed curves*) and $\tau_T = 2$ (*dotted curves*). The notch at 7 keV is due to Fe K-edge absorption. For comparison, the solid curves depict the reflection spectra from a cold, semi-infinite slab. Note the close similarity of the composite spectra in the disk and torus geometry.

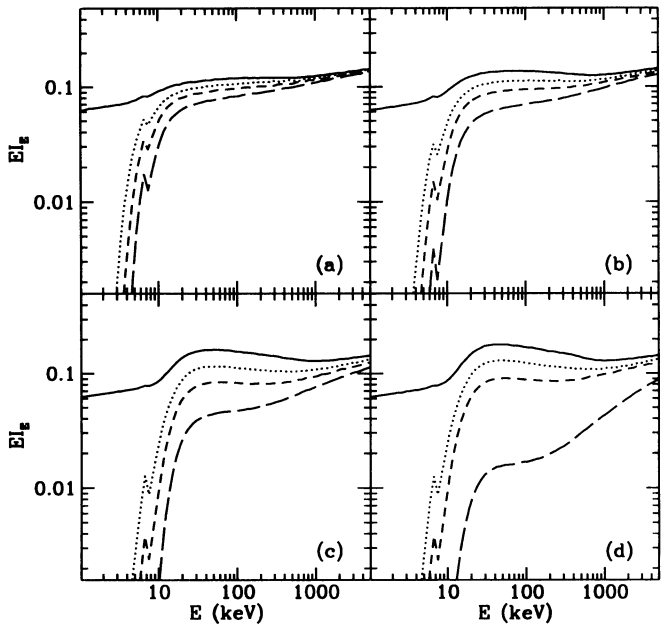

FIG. 2.—Composite spectra for different angles, θ, of inclination between the symmetry axis of the torus and the line of sight. Solid, dotted, short-dashed, and long-dashed curves are computed for $\theta = 5°$ (nearly pole-on view), 35°, 55°, and 85° (nearly edge-on view), respectively. The simulations illustrated in Figs. 2*a*–2*c* all used tori with square cross sections: (*a*) $\tau_T = 0.5$; (*b*) $\tau_T = 1$; (*c*) $\tau_T = 2$; (*d*) spectrum emerging from a rectangular torus whose radial and vertical optical depths are 4 and 2, respectively.

roughly isotropic. The three simulations illustrated in Figures 2*a*–2*c* all used tori with square cross sections, differing only in optical depth. When $\tau_T \lesssim 2$, the fraction of the incident photons striking the torus which is scattered rises steadily with τ_T, making the amplitude of the bump grow with increasing τ_T. This effect saturates for larger τ_T; when $\tau_T \gtrsim 2$, nearly all the incident photons are scattered independent of the actual value of τ_T. Finally, when τ_T is larger than several, the amplitude of the bump is reduced again because of Compton losses at all energies.

The flux in unobscured directions also depends weakly on torus cross section. Figure 2*d* shows the spectrum emerging from a rectangular torus whose Thomson optical depth along the equatorial direction is 4 while its optical depth in the vertical direction is 2. The amplitude of the bump is increased relative to the square $\tau_T = 2$ case (Fig. 2*c*) by slightly more than the increased optical depth would indicate; this is because the rectangular cross section makes it somewhat more likely for scattered photons to leave through the top or bottom surfaces than through the outer surface.

4. OBSCURED VIEWS

As shown by Madau et al. (1993), the X-ray flux is subject to suppression at all energies when viewed from an obscured direction. Because the low-energy cutoff is a true absorption effect, its magnitude depends exponentially on

$$\tau_{\rm eff}(x) = \sqrt{\tau_{\rm abs}(x)[\tau_{\rm abs}(x) + \tau_T]}\,,$$

where $\tau_{\rm abs}(x)$ is the energy-dependent photoelectric opacity at energy x. Incident photons with energies $x \gtrsim 1$ are instead downscattered to lower energies: this makes the spectrum harder than the original for $x > 0.4$.

When $\tau_T \lesssim 1$, the only significant alteration of the X-ray flux is due to standard soft X-ray absorption, but of particularly large magnitude. For larger values of τ_T, photoelectric absorption is enhanced by scattering: the energy below which photons are absorbed $x_{\rm co}$ increases $\propto \tau_T^{2/3}$ rather than the usual $x_{\rm co} \propto \tau_T^{1/3}$.

When $\tau_T \gtrsim 1$, photons of all energies are removed from obscured viewing angles. Because the electron scattering cross section is independent of photon energy for $x \lesssim 0.2$, the entire range of energies from 20 keV (where Fe K edge opacity becomes negligible) to $\simeq 100$ keV (the beginning of the Klein-Nishina regime) is affected in the same way. Whether photons leave through the top or bottom surfaces of the torus, or through the outer surface, depends on a combination of the aspect ratio of the torus's cross section and its optical depth. When the torus is square and $\tau_T \sim 1$ (Figs. 2*b* and 2*c*), the probability for emergence through the outer surface is not much less than through the top, so the flux is depressed by only $\simeq 50\%$ to a factor of 2. By contrast, when the torus horizontal thickness is significantly greater than its vertical thickness (Fig. 2*d*), the probability of escape out the top or bottom is significantly greater than for escape out the outermost surface, and the flux in the equatorial plane is reduced by a larger factor than if the optical depth had been increased to 4 in both directions.

5. IRON Kα LINE

We have also computed the equivalent width (EW) of the Kα line produced in the torus as a function of the viewing angle (see Awaki et al. 1991).

For unobscured views the EW is rather similar to that resulting from disk reflection models (George & Fabian 1991; Matt, Perola, & Piro 1991). The Kα line equivalent width has a characteristic value of ~ 100 eV for $\tau_T = 0.5$–1, in broad agreement with the values observed by *Ginga* in a large fraction of the detected Seyfert 1 galaxies. The EW decreases to 55 eV when $\tau_T = 2$, increases slightly when the torus is elongated in the radial direction, and decreases slightly with increasing torus half-opening angle. While we expect these trends to be robust, we also expect that the actual value of the EW in unobscured directions could be altered by as much as a factor of 2 by changes in the shape of the torus inner edge.

A wider range of EW, which is very sensitive to geometry and optical depths, is seen in obscured views. Both line and continuum are absorbed, but line photons less so as they originate more or less uniformly within the torus. The Kα line is therefore much stronger relative to the continuum, with an equivalent width ranging, in the equatorial plane, from 280 eV for $\tau_T = 0.5$ to 3.7 keV for $\tau_T = 2$. Note that any warm, scattering material above the axis of the obscuring torus, not included in our calculations, will also contribute to the continuum and Fe Kα line flux, but the torus and scattering contributions can be distinguished by the energy of the line: in the torus the Fe is at most weakly ionized, while in the scattering region it should be highly ionized (Krolik & Kallman 1987). Marshall et al. (1993) found that the Fe Kα flux in NGC 1068 is split roughly equally between "cold" and ionized stages; it is possible that the torus and the reflection region contribute comparably.

6. DISCUSSION

These results have consequences for three different subject areas: interpretation of X-ray spectra (or upper limits) for type 2 Seyfert galaxies; interpretation of the bump and the iron Kα

line observed in the X-ray spectra of type 1 Seyferts; and the origin of the X-ray background. We discuss each subject in turn.

The large, but measurable, column densities seen in some type 2 Seyfert galaxies by Awaki & Koyama (1994) and Mulchaey et al. (1992) have an easy interpretation within this picture: they are cases in which the torus either is relatively thin, or in which our line of sight cuts a corner. The fraction of all type 2 Seyferts in which the line of sight column density is $\lesssim 10^{24}$ cm^{-2}, is, of course, a function of the torus optical depth; these would be rare if $\tau_T \gtrsim 3$. It is also worth noting that the Mulchaey et al. sample, in which relatively small column densities were typically found, was drawn from an ultraviolet survey. As shown by Balsara & Krolik (1993), the fraction of the nuclear light reflected by warm ionized gas rises very sharply as the viewing angle moves out of the plane. Consequently, it is not surprising that an ultraviolet-selected sample should have preferentially smaller column densities.

Other cases, such as NGC 1068, in which the hard X-ray flux appears to be suppressed by a factor $\gtrsim 50$ (Cameron 1993, private communication) present stronger constraints. In these objects, if τ_T is only a few, the torus must be considerably optically thicker in the horizontal direction than in the vertical, and our line of sight cannot be too far out of the equatorial plane. In the case of NGC 1068, this last requirement is also imposed by the large velocity shifts seen in reflected optical emission lines (Balsara & Krolik 1993) and supported by the shape of the infrared spectrum (Pier & Krolik 1993). If τ_T is rather greater, the aspect ratio is less strongly constrained. Since the greatest suppression factor at 60 keV found in any of our calculations was about 30 (for equatorial views and a square cross section torus with $\tau_T = 8$), a larger constrast between the horizontal and vertical sizes and/or a larger depth are necessary to explain the OSSE upper limits. More hard X-ray observations of type 2 Seyferts (perhaps by OSSE) will clarify what the distribution of τ_T (and aspect ratio) really is.

We have also shown that production of a bump above 10 keV in the spectra of unobscured Seyfert galaxies, along with a Fe Kα line with equivalent width ~ 100 eV, are an immediate consequence of the existence of an obscuring torus blocking a significant fraction of solid angle around the nucleus and having a Thomson depth of order unity. Although we have not fit any of our models to actual data, the close resemblance between our bump features and those predicted by disk reflection models makes it difficult to distinguish the two models solely on the basis of fits to X-ray spectral data. To the degree that the existence of an obscuring torus is well-established (e.g., from the presence of an ionization cone, or strong nuclear mid-infrared flux), *one might be able to explain any X-ray bump and* Fe Kα *line in type 1 Seyfert galaxies soley by reflection and fluorescence from the torus, and dispense with any disk reflection component.*

In at least one type 1 Seyfert, NGC 4151, there is no evidence for a 20–30 keV bump. Interestingly, *HST* and HUT observations of NGC 4151 (Evans et al. 1993; Kriss et al. 1992) show that the obscuration in this galaxy takes an unusual form: the material which defines the ionization cones is optically thick at the Lyman edge but optically thin to dust extinction in the ultraviolet. It may or may not sandwich a core which is optically thick to dust extinction. The opening angle of the material with little extinction is $35° \pm 10°$, similar to the opening angle of the tori in our calculations. Because material with a normal dust/gas ratio that is optically thick to X-rays has a very large extinction, the opening angle of the material optically thick to X-rays in NGC 4151 must be rather larger. Our model would then predict an unusually weak bump in NGC 4151. It is also possible that even in the equatorial plane the column density is as small as in the subset of type 2 Seyfert galaxies observed by Mulchaey et al. (1992).

The clearest experimental test to distinguish between these two scenarios is a search for variability in these features. If the bump and line fluxes vary on any timescale much shorter than a few years, their origin must lie in a structure closer to the nucleus, such as the innermost regions of an accretion disk. Conversely, if the bump and line fluxes stay constant despite changes in the underlying power law, that would be strong evidence in favor of a more distant origin for the reprocessing region, such as an obscuring torus. To date, there is only marginal evidence for variability of the reflection component in NGC 5548 (Nandra et al. 1991). In one object, NGC 6814, variability in the Kα line on few minute timescales has been reported (Kunieda et al. 1990); however, recent observations have shown this variability to be a spurious effect due to confusion (Madejski et al. 1993). No evidence for variability of the iron Kα line has been found in NGC 4151 (Yaqoob & Warwick 1991).

A second distinction between reflection close in and transmission through the torus may lie in the Fe Kα profile. Fe Kα from the torus should be narrow, ~ 100 km s^{-1}, while Fe Kα from the accretion disk may be broadened both by the large orbital velocities in the inner disk and by a possible range in ionization stages.

Finally, as pointed out by Madau et al. (1993) and Zdziarski, Życki, & Krolik (1993), our current view of the shape of Seyfert X-ray spectra makes it very likely that AGNs with obscuring tori are the dominant contributors to the X-ray background. Because the reflection bump produces a comparatively hard spectrum in the energy range 2–30 keV, the reprocessing of X-ray photons in obscuring tori may play an important role in shaping the X-ray background spectrum, particularly if this structure exists in high-redshift quasars as well as in low-redshift Seyfert galaxies.

We thank C. Done and G. Madejski for discussing with us their unpublished data on NGC 6814, and B. Czerny and A. Zdziarski for useful conversations. J. H. K. is supported by NASA grant NAGW 3129 and PTZ supported in part by grant 2 P304 010 04 financed in 1993–1995 by the State Committee for Scientific Research. After this work was largely completed, we discovered that G. Ghisellini, F. Haardi, and G. Matt had independently come to similar conclusions.

REFERENCES

Antonucci, R. R. J. 1993, ARA&A, 31, 473
Antonucci, R. R. J., & Miller, J. S. 1985, ApJ, 297, 621
Awaki, H., & Koyama, K. 1994, in Proc. COSPAR Symp. on Recent Results in X-Ray and EUV Astronomy, in press
Awaki, H., Koyama, K., Ionue, H., & Halpern, J. P. 1991, PASJ, 43, 195
Balsara, D., & Krolik, J. H. 1993, ApJ, 402, 109
Cameron, R. A., et al. 1994, in Proc. Compton Symp., ed. N. Gehrels, in press
Elvis, M., & Lawrence, A. 1988, ApJ, 331, 161
Evans, I. N., Tsvetanov, Z., Kriss, G. A., Ford, H. C., Caganoff, S., & Koratkar, A. P. 1993, ApJ, 417, 82
Fabian, A. C., Nandra, K., Celotti, A., Rees, M. J., Grove, J. E., & Johnson, W. N. 1993, ApJ, 416, L57

George, I. M., & Fabian, A. C. 1991, MNRAS, 249, 352
George, I. M., Nandra, K., & Fabian, A. C. 1990, MNRAS, 242, 28P
Huchra, J., & Burg, R. 1992, ApJ, 393, 90
Jourdain, E., et al. 1992, A&A, 256, L38
Koyama, K., Inoue, H., Tanaka, Y., Awaki, H., Takano, S., Ohashi, T., & Matsuoka, M. 1989, PASJ, 41, 731
Kriss, G. A., et al. 1992, ApJ, 392, 485
Krolik, J. H., & Kallman, T. R. 1987, ApJ, 320, L5
Kunieda, H., Turner, T. J., Awaki, H., Koyama, K., Mushotzky, R., & Tsusaka, Y. 1990, Nature, 345, 786
Leahy, D. A., & Creighton, J. 1993, MNRAS, 263, 314
Lightman, A. P., & White, T. R. 1988, ApJ, 335, 57
Madau, P., Ghisellini, G., & Fabian, A. C. 1993, ApJ, 410, L7
Madejski, G. M., Done, C., Turner, T. J., Mushotzky, R. F., Serlemitsos, P., Fiore, F., Sikora, M., & Begelman, M. C. 1993, Nature, 365, 626
Maisack, M., et al. 1993, ApJ, 407, L61
Marshall, F. E., et al. 1993, ApJ, 405, 168
Matsuoka, M., Piro, L., Yamauchi, M., & Murakami, T. 1990, ApJ, 361, 440
Matt, G., Perola, G. C., & Piro, L. 1991, A&A, 247, 25
Miller, J. S., & Goodrich, R. W. 1990, ApJ, 355, 456
Morrison, R., & McCammon, D. 1983, ApJ, 270, 119
Mulchaey, J. S., Mushotzky, R. F., & Weaver, K. A. 1992, ApJ, 390, L69
Nandra, K., Pounds, K. A., Stewart, G. C., George, I. M., Hayashida, K., Makino, F., & Ohashi, T. 1991, MNRAS, 248, 760
Osterbrock, D. E., & Shaw, R. A. 1988, ApJ, 327, 89
Phillips, M. M., Charles, P. A., & Baldwin, J. A. 1983, ApJ, 266, 485
Pier, E. A., & Krolik, J. H. 1993, ApJ, 417, L23
Piro, L., Yamauchi, M., & Matsuoka, M. 1990, ApJ, 360, L35
Pogge, R. W. 1988, ApJ, 328, 519
Pounds, K. A., Nandra, K., Stewart, G. C., George, I. M., & Fabian, A. C. 1990, Nature, 344, 132
Pozdnyakov, L. A., Sobol', I. M., & Sunyaev, R. A. 1983, Ap&SS, 2, 189
Wilson, A. S., Ward, M. J., & Haniff, C. A. 1988, ApJ, 334, 121
Yaqoob, T., & Warwick, R. S. 1991, MNRAS, 248, 773
Zdziarski, A. A., Życki, P. T., & Krolik, J. H. 1993, ApJ, 414, L81